

Miscibility of PVDF/PMMA blends examined by crystallization dynamics

Hozumi Sasaki, Palash Kanti Bala, Hirohisa Yoshida* and Eiko Ito

Department of Industrial Chemistry, Tokyo Metropolitan University, Minami Osawa,
Hachioji-shi, Tokyo 192-03, Japan

(Received 24 October 1994; revised 28 April 1995)

The crystallization dynamics of blends of poly(vinylidene fluoride) (PVDF) with atactic-, syndiotactic- and isotactic-poly(methyl methacrylate)s (PMMA) were analysed by differential scanning calorimetry under isothermal conditions. Crystal growth rate (G) decreased with increasing weight fraction of PMMA (ϕ_{PMMA}) for PVDF/at-PMMA and PVDF/syn-PMMA blends. However, G of PVDF/iso-PMMA blends depended only on the degree of supercooling (ΔT) and was independent of ϕ_{PMMA} . Surface free energy (σ) of PVDF crystals evaluated from G and nucleation rate depended on ϕ_{PMMA} for PVDF/at-PMMA and PVDF/syn-PMMA blends, although σ of PVDF/iso-PMMA was almost constant and independent of ϕ_{PMMA} . These results suggest that PVDF/at-PMMA and PVDF/syn-PMMA blends are miscible but PVDF/iso-PMMA blends are immiscible, a finding which was confirmed by the phase diagrams as determined from cloud point measurements.

(Keywords: PVDF/PMMA blends; miscibility; crystallization dynamics)

INTRODUCTION

Poly(vinylidene fluoride) (PVDF)/poly(methyl methacrylate) (PMMA) blends, one example of crystalline/amorphous polymer blends, are miscible in the molten state¹. Many studies of this blend have been carried out from both scientific and technological viewpoints^{1–8}. The miscibility of PVDF/PMMA blends is thought to be a result of interaction between the oxygen atom of carbonyl groups of PMMA and the hydrogen atom of PVDF³. Several studies have been carried out on blends of PVDF and isotactic-, syndiotactic- and atactic-PMMA. Roerdink and Challa⁴ reported the influence of tacticity of PMMA on the compatibility with PVDF, based on observations of glass transition temperature (T_g) and melting temperature (T_m) depressions. Riedl and Prud'homme⁵ evaluated the polymer–polymer interaction parameter (χ_{12}) for PVDF/PMMA with different tacticity using T_m depression data⁴. Both reports suggest that blends of PVDF and isotactic-, syndiotactic- and atactic-PMMA are miscible, although each blend exhibits a different interaction parameter.

It is well known that PVDF is able to form six different crystal modifications, I(β), II(α), III(γ), IV, V and VI, corresponding to molecular conformation and packing. The most stable modification, II(α), is obtained upon cooling from the melt. Leonard *et al.*⁶ reported that the I(β) modification of PVDF is observed upon annealing of PVDF/PMMA blends over a composition range that depends on PMMA tacticity, due to the change of crystallization behaviour. We have also observed

selective crystallization of the I(β) modification in PVDF/PMMA blend systems with PMMA weight fraction (ϕ_{PMMA}) in the range from 0.2 to 0.4, depending on PMMA tacticity⁹. However, the values of χ_{12} for PVDF/PMMA blends estimated from the equilibrium melting temperature (T_m°) depression increase in the order atactic, syndiotactic and isotactic⁹. The χ_{12} value (-0.02) of PVDF/iso-PMMA suggests that the mixing state of PVDF/iso-PMMA in the melt is metastable⁹, which differs from the results of other researchers^{4,5}. Recently, Takahashi *et al.*¹⁰ pointed out that the χ_{12} value obtained from melting temperature depression using the Nishi–Wang equation¹¹ contained large errors compared with values obtained by other methods. As the applicability of the Hoffman–Weeks plot¹² to determine T_m° is expected to be limited, especially for polymers showing polymorphism such as PVDF, we have studied the kinetics of isothermal crystallization from the melt to estimate the miscibility of crystalline/amorphous polymer blends.

In this study, the interaction and miscibility between PVDF and PMMA with different tacticity were estimated from crystallization dynamics, including the dependence of the crystal growth rate (G) and the surface free energy (σ) of PVDF crystals on ϕ_{PMMA} . The following assumptions were made. In a miscible blend, the crystallization of PVDF is obstructed by mixing with PMMA, and G of PVDF depends on ϕ_{PMMA} . On the other hand, in an immiscible blend, the crystallization of PVDF is not influenced by mixing with PMMA because the PVDF phase separates from the PMMA phase. In this way, interaction and miscibility can be estimated by investigating the ϕ_{PMMA} dependence of G . Furthermore, the σ value of the PVDF crystals in the blends depends

* To whom correspondence should be addressed

on the concentration of PMMA in the amorphous region around crystallites. In a miscible blend, this PMMA concentration is thought to be equal to ϕ_{PMMA} ; therefore σ is expected to depend on ϕ_{PMMA} . In an immiscible blend, as crystallization occurs in the PVDF phase, the PVDF crystal is surrounded by amorphous PVDF; therefore σ should be a constant and independent of ϕ_{PMMA} .

EXPERIMENTAL

Samples

PVDF supplied by Kureha Chemical Co., Ltd, at-PMMA supplied by Mitsubishi Resin Co., Ltd, and ionic polymerized iso- and syn-PMMA reported previously¹³ were used in this study. Characteristics of the PVDF and PMMA are shown in Table 1. PVDF and PMMA were dissolved in *N,N*-dimethylacetamide at room temperature. The blend composition is indicated by the weight fraction of PMMA ($\phi_{\text{PMMA}} = 0.4$ indicates the blend of composition PVDF/PMMA = 0.6/0.4). Blend samples were obtained by solvent casting on a glass plate at 333 K in a desiccator. The obtained blend films were further dried under vacuum at room temperature for 3 days.

Cloud point measurements

Cloud points were measured using an apparatus assembled in our laboratory comprising a semiconductor laser (Applied Opt-Olanning Inc., model STK-M, $\lambda = 670$ nm, 1.0 mW), a photodiode (Hamamatsu Photonics Co., Ltd, model S-1226) and an instrument capable of simultaneous thermal analysis and small-angle X-ray scattering measurement (d.s.c./SAXS)^{14,15} on the flat optical bench. The cast film sample sandwiched between cover glasses was set in the sample holder of the d.s.c./SAXS instrument, which was connected to a Seiko thermal analysis station SSC5200H. The sample was irradiated by passing the laser beam through the 2 mm diameter window of the d.s.c./SAXS instrument, and the transmitted light intensity was measured by the photodiode. The d.s.c./SAXS instrument was scanned at 10 K min⁻¹ from room temperature to 650 K under a dry nitrogen gas atmosphere. The d.s.c. signal and the transmitted light intensity were measured as a function of temperature.

Isothermal crystallization

Isothermal crystallization was carried out using a Seiko differential scanning calorimeter (DSC200) connected to a Seiko thermal analysis system SSC5200H. The sample was heated to 473 K and maintained at that

temperature for 3 min, then quenched to a predetermined crystallization temperature (T_c). The heat of crystallization at T_c was measured until the crystallization was complete. Two characteristic times were evaluated from the exothermic d.s.c. peak: the time from quenching to T_c to the start of the exothermic peak due to crystallization (T_{st}) and the time from T_{st} to when 50% of the crystallization had occurred, denoted T_n and $T_{(0.5)}$, respectively¹⁶. The reciprocals of T_n and $T_{(0.5)}$ were employed as the nucleation rate (N) and the crystal growth rate (G). Temperature variation during crystallization was at most ± 0.5 K. Isothermal crystallization was carried out at various T_c values, and runs in which crystallization occurred before T_c was reached were eliminated. After crystallization, samples were quenched to room temperature, and T_m was measured at 10 K min⁻¹.

RESULTS AND DISCUSSION

Phase diagram

The simultaneous thermal analysis and light transparency results of PVDF/syn-PMMA with $\phi_{\text{PMMA}} = 0.3$ are shown in Figure 1. The transmitted light (TL) intensity increased slightly at the melting peak temperature and decreased rapidly at 553 K. As the laser light was scattered by crystallites in the cast film, the TL intensity was somewhat lower at temperatures below T_m . However, crystallites in the cast film melted completely at the melting peak temperature and the TL intensity increased at temperatures above T_m . With increasing temperature, the d.s.c. base line shifted to the endothermic direction and the TL intensity decreased suddenly at 553 K. When the sample was heated at 563 K, it became slightly opaque without any colour change. Thermal decomposition of PVDF/PMMA blends was found to start at ~ 650 K from thermogravimetric (t.g./d.t.a) measurement. Therefore, the steep decrease of the TL intensity observed at 553 K was due to phase separation.

In the case of PVDF/at-PMMA blends, the steep decrease of TL intensity was observed at temperatures above 630 K. PVDF/at-PMMA blend is reported to exhibit lower critical solution temperature (LCST) behaviour at ~ 620 –630 K (refs 17, 18). However, it

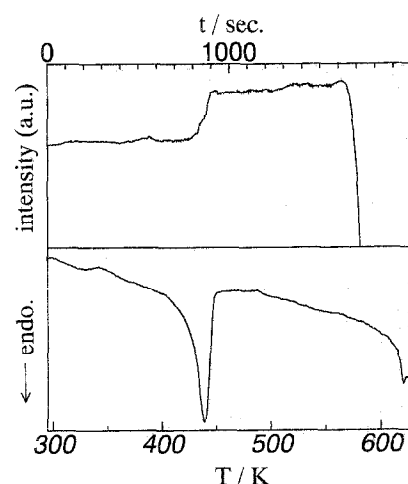


Figure 1 Simultaneous measurement of d.s.c. (top) and transmitted light intensity (bottom) for PVDF/syn-PMMA with $\phi_{\text{PMMA}} = 0.3$

Table 1 Characteristics of polymers studied

Polymer	$M_n \times 10^{-5}$	M_n/M_w	N.m.r. triad			T_m (K)	T_g (K)
			[I]	[S]	[H]		
PVDF	26.0	—	—	—	—	453 ^a	239
at-PMMA	1.5	1.5	0.13	0.43	0.44	—	376
syn-PMMA	2.0	1.2	0.20	0.60	0.20	—	382
iso-PMMA	1.6	1.7	0.93	0.03	0.04	—	317

^a α -Modification

was difficult to assign the steep decrease of TL intensity observed in PVDF/at-PMMA blend to either phase separation or thermal decomposition. For PVDF/syn-PMMA and PVDF/iso-PMMA blends, the steep decrease of TL intensity was observed in the temperature range between T_m and 600 K: this temperature depended strongly on ϕ_{PMMA} for the PVDF/syn-PMMA blend system but was observed immediately after T_m in the case of PVDF/iso-PMMA. As both blend systems contained some crystallites, the TL intensity increased after T_m . However, the TL intensity at temperature immediately after T_m of PVDF/iso-PMMA blend was approximately one order of magnitude lower than that of the PVDF/syn-PMMA blend. This fact suggests that PVDF/iso-PMMA is already phase-separated below T_m .

T_m and cloud point, determined as the intersection of the TL base line at the temperature range above T_m and the slope of the steep decrease of TL intensity, which corresponded to the LCST line, are plotted against ϕ_{PMMA} for PVDF/syn-PMMA and PVDF/iso-PMMA blends in Figure 2. The LCST line of PVDF/iso-PMMA overlapped with the T_m line in the ϕ_{PMMA} range between 0.3 and 0.7. This result suggests that the PVDF/iso-PMMA blend with ϕ_{PMMA} ranging from 0.3 to 0.7 is in the phase-separated state. On the other hand, the LCST line of PVDF/syn-PMMA existed at temperatures above $T_m + 50$ K. The reported LCST line of PVDF/at-PMMA exists at temperatures far from the T_m line^{17,18}. Thus even though they are both miscible systems, the phase behaviour of the PVDF/syn-PMMA blend differed from that of the PVDF/at-PMMA blend. Phase diagrams observed in this study showed good agreement with the order of reported χ_{12} values for PVDF/PMMA with different tacticity, except for the large negative value for the PVDF/iso-PMMA blend^{4,5}.

Crystal growth rate

The relationship between the degree of supercooling ($\Delta T = T_m - T_c$) and the crystal growth rate (G) for each blend system is shown in Figures 3a–c. G of all the blends became the faster with increasing ΔT . It is well known that G versus ΔT plots show a maximum between T_m

and T_g , because the diffusion of molecules is restricted due to high viscosity at large ΔT ¹⁹. In this study, however, data at high ΔT were neglected since this led to crystallization of the samples before T_c was reached.

For the PVDF/at-PMMA blend shown in Figure 3a, G decreased with increasing ϕ_{PMMA} at the same ΔT . The temperature dependence curve of G shifted to the large ΔT side with increasing ϕ_{PMMA} . Crystallization of polymers proceeds via two processes: diffusion and absorption of the crystalline polymer on the crystal growth surface²⁰. In PVDF/PMMA, it is reported that diffusion control of PVDF crystallization occurs in blends with PMMA having $M_w > 6 \times 10^3$ and that the α -form of PVDF crystals forms selectively under such crystallization conditions²¹. Therefore, these results indicate that the diffusion of PVDF is obstructed by mixing with at-PMMA. In the PVDF/syn-PMMA blend shown in Figure 3b, as well as in the PVDF/at-PMMA blend, G decreased with increasing ϕ_{PMMA} in the same T_c range. The phase diagram shown in Figure 2 suggested that this blend system was also miscible within the experimental conditions for crystallization. For PVDF/syn-PMMA blend, however, the ϕ_{PMMA} dependence of the G versus ΔT plots was weaker than that of the PVDF/at-PMMA blend; in other words, the ΔT range of crystallization in PVDF/syn-PMMA was smaller than that in PVDF/at-PMMA at a given ϕ_{PMMA} .

In the PVDF/iso-PMMA system shown in Figure 3c, G of the blend with $\phi_{\text{PMMA}} = 0.1$ is slightly faster and G of the blend with $\phi_{\text{PMMA}} = 0.4$ is slower than that of pure PVDF at a given ΔT . In the ϕ_{PMMA} range between 0.1 and 0.4, however, G of PVDF/iso-PMMA blend was independent of ϕ_{PMMA} in the same ΔT range. As can be seen in Figure 2, the melt at 473 K of PVDF/iso-PMMA with ϕ_{PMMA} range between 0.1 and 0.4 was in the two-phase region. Before the samples reached T_c , phase separation proceeded in this system except for the blend with $\phi_{\text{PMMA}} = 0.1$. As PVDF/iso-PMMA blends were completely phase-separated in the melt or at T_c , G depended only on ΔT and was independent of the ϕ_{PMMA} .

The ΔT range, in which isothermal crystallization was observable, shifted to the large ΔT side in the order iso-, syn- and at-PMMA at a given ϕ_{PMMA} . It is expected that G is influenced by changes of T_m and T_g with ϕ_{PMMA} . However, the T_m difference between PVDF/at-PMMA and PVDF/iso-PMMA at $\phi_{\text{PMMA}} = 0.4$ was at most 5 K, which was the largest T_m difference in this study, and T_g values were below room temperature for all blends in this ϕ_{PMMA} range from 0 to 0.4. Therefore, we conclude that differences in G arise from changes in phase behaviour and not from changes of T_m and T_g with ϕ_{PMMA} .

Within the experimental conditions PVDF/syn-PMMA and PVDF/at-PMMA blends were miscible, yet showed a different relationship between G and ΔT at a given ϕ_{PMMA} . The tendency may be explained by the following two hypotheses. The first interpretation is that diffusion of PVDF is weakly obstructed by syn-PMMA compared with at-PMMA at the same ϕ_{PMMA} , since the interaction between PVDF and syn-PMMA is weaker than that between PVDF and at-PMMA considering χ_{12} . The other is that concentration fluctuations exist in the PVDF/syn-PMMA blend and the PVDF crystallizes in a relatively lower PMMA concentration even at the same ϕ_{PMMA} . As shown in Figure 2, isothermal

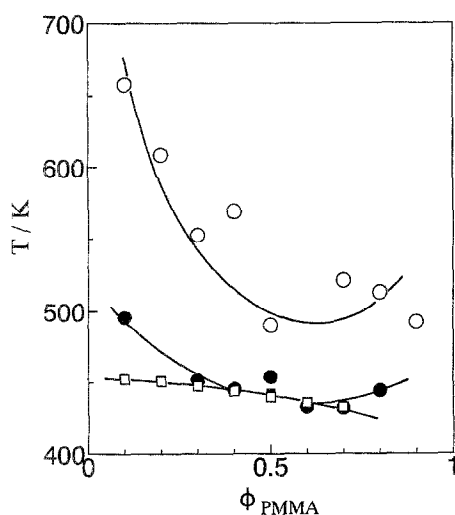


Figure 2 ϕ_{PMMA} dependency of T_m (□) and cloud point of PVDF/syn-PMMA (○) and PVDF/iso-PMMA (●)

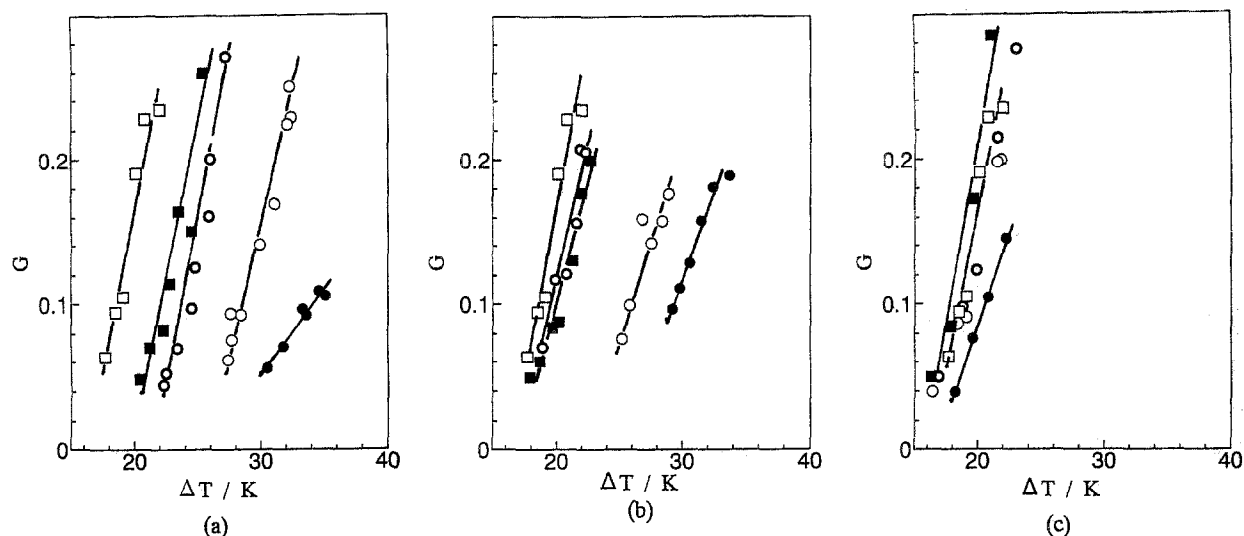


Figure 3 Crystal growth rate G in PVDF and PVDF/at-PMMA (a), PVDF/syn-PMMA (b) and PVDF/iso-PMMA (c) blends with $\phi_{\text{PMMA}} = 0$ (\square), 0.1 (\blacksquare) 0.2 (\odot), 0.3 (\circ) and 0.4 (\bullet) at various isothermal crystallization temperatures (T_c)

crystallization carried out at T_c by quenching from the melt at 473 K which was closer to the $LCST$ line in the case of PVDF/syn-PMMA blend than in PVDF/at-PMMA blend. Since weak interaction may be a result of concentration fluctuations in the PVDF/syn-PMMA blend, the difference between Figures 3a and b is thought to appear by both effects. Despite the PVDF/syn-PMMA blends being miscible, concentration fluctuations and/or a weak interaction between PVDF and syn-PMMA existed in this system.

According to Lauritzen and Hoffman²², when T_c is close to the melting point, the temperature dependence of G may be written as

$$G = G^0 \exp(-\Delta E/RT_c - K_g/RT_c \Delta T) \quad (1)$$

where G^0 , ΔE and R are, respectively, a constant that is independent of temperature, the activation energy of diffusion and the gas constant. K_g is a nucleation factor given by

$$K_g = nbT_m \sigma / \Delta H_m^2 \quad (2)$$

where n , b and ΔH_m are a constant that depends on regime, the length of stem and the heat of melting, respectively. σ is called the average surface free energy and is given as

$$\sigma = \sigma_u^2 \sigma_e \quad (3)$$

where σ_u and σ_e indicate lateral surface free energy and fold surface free energy, respectively.

The plot of $\log G$ versus $1/T_c \Delta T$ is generally used for analysis of the temperature dependence of G , and the slope of the plot is used to determine the regime²³. The relationship between $\log G$ and $1/T_c \Delta T f$ for each blend is shown in Figures 4 a–c, in which f is a correction factor given by $f = 2T_c/(T_m + T_c)$ that considers the temperature dependence of ΔH_m in K_g shown in equation (2). Plots of each blend became one straight line at a given ϕ_{PMMA} , and the regime transition was not observed in this temperature range. Saito *et al.*¹⁸ reported the regime transition in PVDF/at-PMMA blend when analysing spherulite crystallization rate using a microscope. We have also reported similar results during analysis of the

isothermal crystallization process of PVDF/at-PMMA and PVDF/syn-PMMA blends using d.s.c.²⁴. When the data at low T_c (in which crystallization starts before the temperature reaches T_c) are added to these plots, another straight line is observed, indicating the existence of the regime transition from regime I to regime II for PVDF/at-PMMA and PVDF/syn-PMMA blends²⁴. This result suggests the possibility that the regime transition is detected as an artefact when data observed under non-isothermal conditions are included in the plots of $\log G$ versus $1/T_c \Delta T$.

Surface free energy

According to the Turnbull–Fisher equation²⁵, the temperature dependence of G may be written as

$$\log G + \Delta E/RT_c = G^0 - KT_m^2/T_c \Delta T^2 \quad (4)$$

where

$$K = 8\pi\sigma/R\Delta H_m^2 \quad (5)$$

Plots of the left-hand side of equation (4) versus $T_m^2/T_c \Delta T^2$ for each blend are shown in Figures 5a–c. Linear relationships are observed for each blend at all compositions, and the values of K were evaluated from each slope shown in Figure 5.

In addition according to Turnbull and Fisher, the temperature dependence of the nucleation rate (N) is given by

$$\log N = N^0 - ST_m^2/T_c \Delta T^2 \quad (6)$$

where

$$S = A[2\sigma/R\Delta H_m^2 - T \log(\nu_{\text{PMMA}})\sigma_e/\Delta H_m^2] \quad (7)$$

and N^0 , A and ν_{PMMA} are, respectively, a constant that is independent of temperature, a constant that depends on both nucleation and crystal growth processes, and the volume fraction of PMMA. Usually $\sigma_u \gg \sigma_e$ and so S is almost proportional to σ . The relationship between $\log N$ and $T_m^2/T_c \Delta T^2$ for each blend is shown in Figures 6a–c, with a linear relationship being observed for all blends and all compositions. The values of S were evaluated from each slope shown in Figure 6.

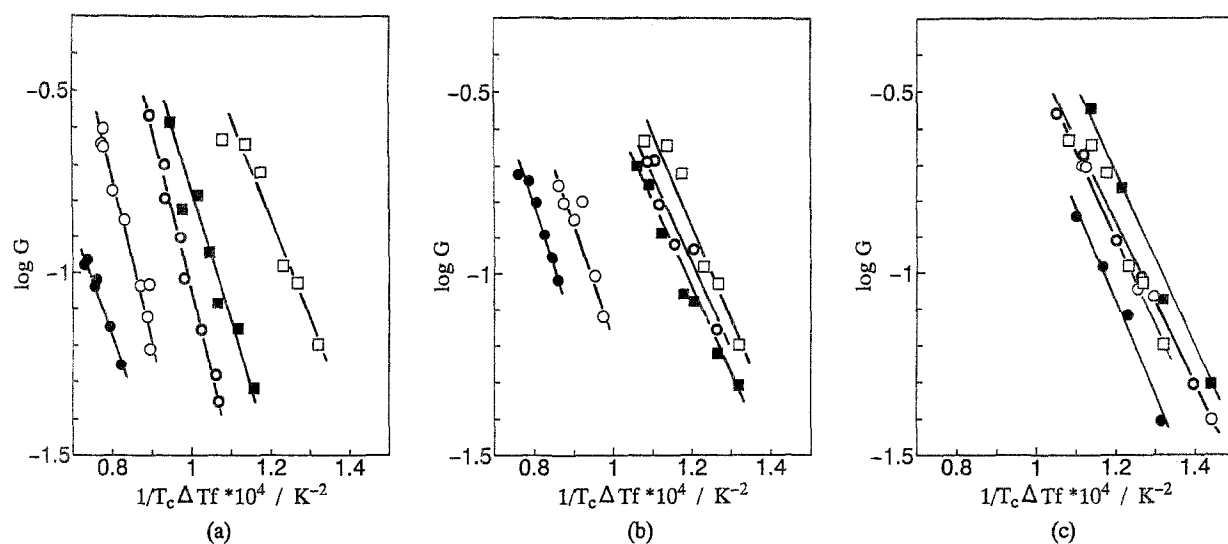


Figure 4 Relationship between $\log G$ and $1/T_c\Delta T_f$ for PVDF and PVDF/at-PMMA (a), PVDF/syn-PMMA (b) and PVDF/iso-PMMA (c) blends with $\phi_{\text{PMMA}} = 0$ (□), 0.1 (■), 0.2 (⊙), 0.3 (○), and 0.4 (●)

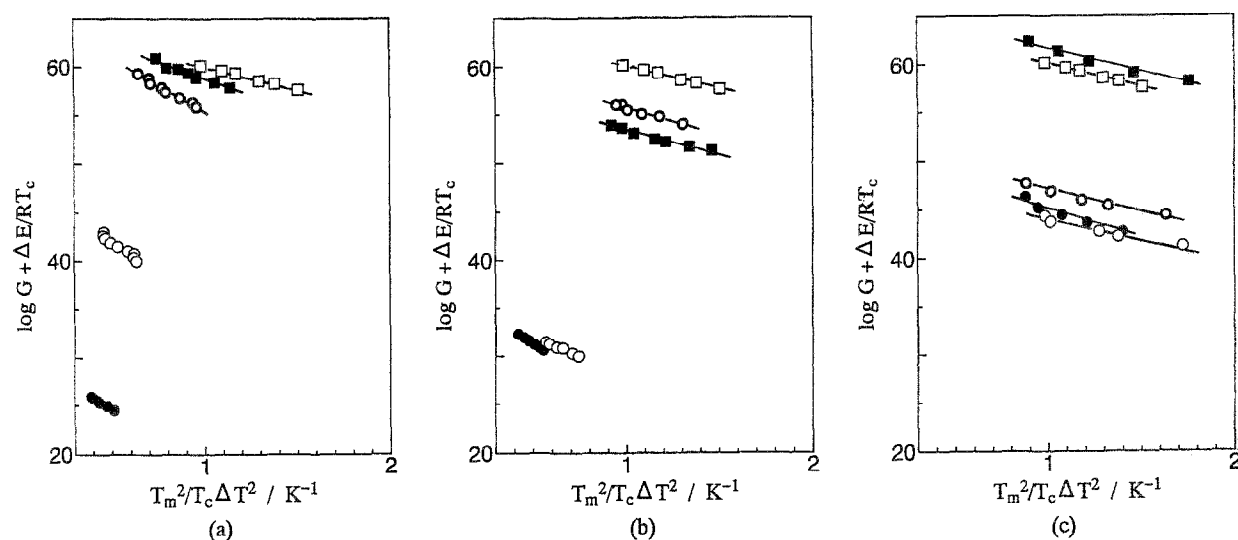


Figure 5 Relationship between $\log G + \Delta E/RT_c$ and $T_m^2/T_c\Delta T^2$ for PVDF and PVDF/at-PMMA (a), PVDF/syn-PMMA (b) and PVDF/iso-PMMA (c) blends with $\phi_{\text{PMMA}} = 0$ (□), 0.1 (■), 0.2 (⊙), 0.3 (○) and 0.4 (●). K values were evaluated from each slope

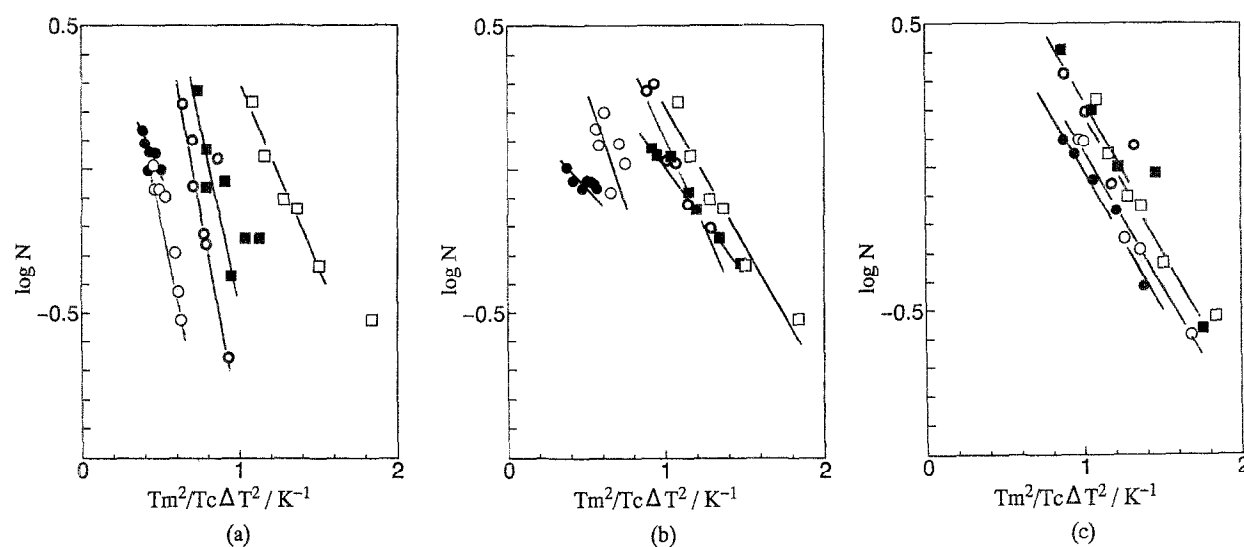


Figure 6 Relationship between $\log N$ and $T_m^2/T_c\Delta T^2$ for PVDF and PVDF/at-PMMA (a), PVDF/syn-PMMA (b) and PVDF/iso-PMMA (c) blends with $\phi_{\text{PMMA}} = 0$ (□), 0.1 (■), 0.2 (⊙), 0.3 (○) and 0.4 (●)

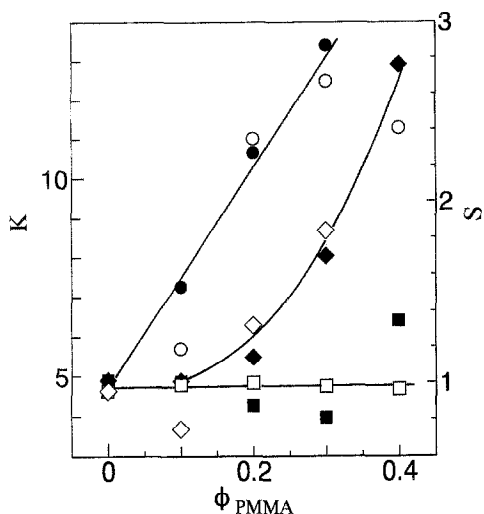


Figure 7 ϕ_{PMMA} dependency of surface free energy terms, K (filled symbols) and S (open symbols), for PVDF/at-PMMA (●, ○), PVDF/syn-PMMA (◆, ◇) and PVDF/iso-PMMA (■, □)

The composition dependences of K and S are shown in Figure 7. K and S showed a good agreement in all blends except that of PVDF/syn-PMMA at $\phi_{\text{PMMA}} = 0.4$. These data are expected to contain some error due to low crystallinity with increasing ϕ_{PMMA} . K and S are proportional to σ as described in equations (5) and (7). In PVDF/at-PMMA blends, σ increased with increasing ϕ_{PMMA} . As σ depends on the PMMA concentration in the amorphous region around the crystal surface, this result indicates that the PMMA concentration changes with increasing ϕ_{PMMA} . In PVDF/syn-PMMA blends, σ increased with increasing ϕ_{PMMA} , but the ϕ_{PMMA} dependency of σ is smaller than that of PVDF/at-PMMA blends. These results suggest that the PMMA concentration in the amorphous region around crystals in PVDF/syn-PMMA may be lower than that in PVDF/at-PMMA blends. Comparing the phase diagrams of PVDF/syn-PMMA and PVDF/at-PMMA, the LCST line of the PVDF/syn-PMMA blend existed at temperature closer to its T_m line. Consequently PVDF/syn-PMMA blends are miscible as discussed above, but concentration fluctuations exist. Therefore, in PVDF/syn-PMMA blends, PVDF crystallizes at regions of low PMMA concentration. For PVDF/iso-PMMA blends, σ was a constant independent of ϕ_{PMMA} . This result suggests that the PMMA concentration in the amorphous region around crystals is constant over the entire ϕ_{PMMA} range examined. Consequently this blend is immiscible and PVDF crystallizes in the PVDF phase.

CONCLUSIONS

It is possible to study the miscibility of crystalline/amorphous polymer blends by analysis of crystallization dynamics. The trends observed in the diffusion process

during isothermal crystallization, as evaluated by G , showed good agreement with the dependence of σ of PVDF crystals on ϕ_{PMMA} , estimated from G and N . The PVDF/iso-PMMA blends used in this study were immiscible, in contrast to previously reported results. The tacticity difference between at-PMMA and syn-PMMA used in this study was not so large as shown in Table 1. However, both blends showed different crystallization dynamics (see Figures 3 and 7). These results indicate that a slight difference in tacticity influences the miscibility of the blends. Therefore, the difference between our results and other reports may be the result of a slight difference in tacticity, especially for the PVDF/iso-PMMA blend. This study also suggests that crystallization dynamics is a sensitive method to determine the miscibility of crystalline/amorphous and crystalline/crystalline polymer blends.

REFERENCES

- 1 Paul, D. R. and Altamirano, J. O. *Adv. Chem. Ser.* 1975, **145**, 371
- 2 Morra, B. S. and Sein, R. S. *J. Polym. Sci., Polym. Phys. Edn* 1982, **20**, 2243
- 3 Leonard, C., Halary, J. L. and Monnerie, L. *Polymer* 1985, **26**, 1507
- 4 Roerdink, E. and Challa, G. *Polymer* 1978, **19**, 173
- 5 Riedl, B. and Prud'homme, R. E. *Polym. Eng. Sci.* 1984, **24**, 1291
- 6 Leonard, C., Halary, J. L. and Monnerie, L. *Macromolecules* 1988, **21**, 2988
- 7 Kaufmann, W., Petermann, J., Reynole, N., Thomas, E. L. and Hsu, S. L. *Polymer* 1989, **30**, 2147
- 8 Gallagher, G. A., Jakeways, R. and Ward, I. M. *J. Polym. Sci., Polym. Phys. Edn* 1991, **29**, 1147
- 9 Takimoto, H., Sato, Y., Yoshida, H., Ito, E. and Hatakeyama, T. *Polym. Prepr., Jpn* 1993, **42**, 1262
- 10 Takahashi, M., Hasegawa, J., Shimono, S. and Matsuda, H. *Netsu sokutei* 1995, **22**, 2
- 11 Nishi, T. and Wang, T. *Macromolecules* 1975, **8**, 909
- 12 Hoffman, J. D. and Weeks, J. J. *J. Res. NBS A* 1962, **66**, 13
- 13 Yoshida, H. and Kobayashi, Y. *Polym. J.* 1982, **14**, 925
- 14 Yoshida, H., Takahashi, M., Hatakeyama, T., Quinn, F. X. and Hatakeyama, H. *PF Activity Report* 1992, **10**, 272
- 15 Yoshida, H., Kinoshita, R. and Teramoto, Y. *Thermochim. Acta* in press
- 16 Kamide, K. and Saito, T. 'Principles and Applications of Thermal Analysis', 3rd Edn, Japan Society of Calorimetry and Thermal Analysis, 1994, p. 67
- 17 Bernstein, R. E., Cruz, C. A., Paul, D. R. and Barlow, J. W. *Macromolecules* 1977, **10**, 681
- 18 Saito, H., Okasa, T., Hamane, T. and Inoue, T. *Macromolecules* 1991, **24**, 4446
- 19 Okui, N. *J. Mater. Sci.* 1990, **25**, 1623
- 20 Keith, H. D. and Padden, F. J. *Polymer* 1986, **27**, 1463
- 21 Braud, D., Jacobs, M. and Hellmann, G. P. *Polymer* 1994, **35**, 706
- 22 Lauritzen, J. I. and Hoffman, J. D. *J. Appl. Phys.* 1973, **44**, 4340
- 23 Hoffman, J. D., Davis, G. T. and Lauritzen, J. I. 'Treatise on Solid State', Plenum Press, New York, 1977, Vol. 3, Ch. 7
- 24 Yoshida, H., Nakamura, H., Takimoto, H., Sasaki, H. and Ito, E. *Rep. Prog. Polym. Phys. Jpn* 1994, **37**, 191
- 25 Turnbull, D. and Fisher, J. C. *J. Chem. Phys.* 1949, **17**, 71